

## An integrated approach of VIKOR and teaching learning based optimization algorithm for milling machinability computations

Shivi Kesarwani<sup>a</sup>, Rajesh Kumar Verma<sup>a\*</sup> and Harshit K. Dave<sup>b</sup>

<sup>a</sup>Materials and Morphology Laboratory, Department of Mechanical Engineering, Madan Mohan Malaviya University of Technology, Gorakhpur, 273010, India

<sup>b</sup>Department of Mechanical Engineering, Sardar Vallabhbhai National Institute of Technology, Surat, 395007, India

### CHRONICLE

#### Article history:

Received: September 14, 2021

Received in revised format:

January 15 2022

Accepted: May 5, 2022

Available online:

May 5, 2022

#### Keywords:

CNO

Nanocomposite

Milling

Surface roughness

VIKOR

TLBO algorithm

### ABSTRACT

The significance of producing Carbon nanomaterials (CNMs) reinforced polymer composites are increasing in manufacturing trades due to their exceptional performances. CNM modified composites are primarily employed in structural component needs due to expanded physico-mechanical properties. This paper highlights a coherent approach of the Višekriterijumsko Kompromisno Rangiranje (VIKOR) and Teaching learning-based optimization algorithm (TLBO) to evaluate the Milling efficiency. The machining was performed for the Milling process of 0-D carbon nano onion (CNO) reinforced polymer (Epoxy) composite at four different levels of Box Behnken Design (BBD). The Milling performances such as Material Removal Rate (MRR) and Surface roughness (SR) were optimized to enhance product quality and productivity. The control of varying process constraints, viz. Weight % of CNO filler content (A), cutting speed (B), feed rate (C) and depth of cut (D), was used to optimize the machining response. The conflicting response is aggregated through the VIKOR method to develop the fitness function for an algorithm. The process constraints play a significant role in influencing the cost and productivity of the machined components. The objective function derived from VIKOR was supplied as input into the TLBO algorithm. The results demonstrated that the spindle speed, feed rate, and weight % of CNO filler are the most contributing factors for machining indices. Also, the hybrid VIKOR-TLBO module shows a lower error percentage than the conventional VIKOR method. The microstructural investigation of the machined surface reveals the feasibility of the proposed hybrid module in a production environment.

© 2022 by the authors; licensee Growing Science, Canada

## 1. Introduction

Polymers play a crucial role in decreasing the structural components weight of aerospace, automobile, defense, and medicinal applications over the last three decades. The exceptional features such as reduced weight, strength, durability, chemical and moisture resistivity make them suitable and more efficient than existing metallic alloys (Andrew et al., 2019; Lau et al., 2006). In polymeric composites, the mechanical characteristic mainly depends upon the reinforcement shape and properties. Moreover, a new trend is remarked to expand the mechanical and physical properties of conventional polymer composites by supplementing nanomaterials. The nanosize addition of the reinforcing material in the matrix phase is performed to control the physio-mechanical properties of the composites for desired functions. Several eminent scholars used different reinforcing materials such as Carbon, Aramid, Basalt, and Glass fibers to boost polymeric material properties (Dhand et al., 2015; Yao et

\* Corresponding author.

E-mail address: [rajeshverma.nit@gmail.com](mailto:rajeshverma.nit@gmail.com) (R. K. Verma)

al., 2016). Fiber/Polymer composites are widely accepted in several sectors, such as mechanical (automotive, aircraft, and aerospace), civil and communication equipment, integrated structures, machinery, textiles, and photoactive materials (Agrawal et al., 2014; Gupta & Srivastava, 2016; Mangalgi, 1999). But these macro fibers reinforced composites have the limitation of high synergistic effects and aspect ratio, and it requires more attention and improvement for high-performance applications. Nanomaterials have effectively fulfilled this gap as a reinforcing agent in the polymer matrix. In nanomaterials, carbon-based fillers such as Carbon nanotubes (CNTs), Carbon Nanorods (CNR), Graphene Nanoplatelets (GNP), and Carbon nano onions (CNOs), etc., are the potential members to augment the biomechanical properties. In order to create advanced tailored materials, different forms of nanoparticles have recently been incorporated into polymer composites (Mittal et al., 2015; Phiri et al., 2017). Nanomaterials have superior mechanical properties, making them cognitive development without altering their strength to improve polymer mechanical properties as additives (Kostagiannakopoulou et al., 2017; Rodríguez-González et al., 2018; Yu et al., 2014). Besides that, the material characteristics found during monotonic loading have not been substantially changed. The shear characteristics of the polymeric materials outside the plane and in-plane are controlled by the matrix property and the reinforcement matrix interface (Chen et al., 2017; Shokrieh & Omid, 2009). Therefore, the matrix mechanical characteristic improvement could indirectly lead to nanomaterial mechanical strength (Jenkins et al., 2019; Kuilla et al., 2010). Polymer matrix deboning induced by the shear load on the ground is one of the significant failure modes for the polymer composites because of stress on the interfaces (Han et al., 2017). In CNMs, spherical shape facilitates better dispersion and low re-agglomeration occurrence leads to improved properties in composites. The epoxy chain mobility under load at 0.1% of fullerene limits elongation at break and tensile strength by 20% (Pikhurov & Zuev, 2014). The alteration of fullerene carbon soot shows a brittle nature, which offers immense benefit for the painting and coating application with corrosion resistance (Pikhurov & Zuev, 2016). The application of fullerene in industrial polymer composites is very low due to high yield synthesis and cost issues. The micro and carbon nanoparticles are prominently used to increase the physio-mechanical characteristics of the polymer matrix. The CNO is a zero-dimensional structure with a high surface area of 10-45nm spherical shape. It is called nano onions due to various concentric layers of the deformed graphite in onion-like shapes. The concentric layers assembly is similar to the onion having noncovalent interactions like van der waal forces (*pie-pie* stacking) between nanoparticles (Dhand et al., 2021; Kristianto et al., 2015). It is broadly used in microwave (Xu et al., 2020), gas storing devices (Raghu et al., 2019), lubrication (Bucholz et al., 2012), biological (Camisasca & Giordani, 2017) functions. It has been remarked from the existing work that very limited data exist on the CNO/ polymer nanocomposite, and the work is limited up to the synthesis and characterization stage only (Bucholz et al., 2012; Camisasca & Giordani, 2017; Dhand et al., 2021; Kristianto et al., 2015; Raghu et al., 2019; Xu et al., 2020).

The component functionally shaped by the product results from the machining process, as a chip produced by the cutting tool interacts with the product surface. The majority of these goods machine the area unevenly and incompletely. A consistent machined surface must be maintained by exploring various machining conditions. Nevertheless, creating a favorable work environment is a challenge because multiple machining factors respond in unique ways during the machining process. Several studies have suggested using different optimization methods to solve various machining tests (Davim & Reis, 2005; Desai & Shaikh, 2012; Richard & Giandomenico, 2018). Several productivity indices are conflicting in nature, such as MRR, tool wear, and surface defects, need to be optimized concurrently during the Milling process (Cheng et al., 2020; Zhou et al., 2017). As a result of considering different process parameters and loading different filler materials in the machining specimens, the authors acknowledged that other machining processes could be completed through various cutting approaches (Taheri-Behrooz et al., 2020). Therefore, a significant issue during the machining is selecting control parameters that satisfy several performance measure criteria. It requires more attraction from material researchers and industries. The CNO reinforced polymers can effectively replace the existing heavyweight metallic materials. But the manufacturing aspect of these polymer nanocomposites is not sufficiently explored in existing research. In industries, the complete utilization of novel material is not possible without knowledge of machining aspects. In machining, various operations are required to assemble the final structure of the developed components. Milling operation is assumed as the primary machining method to create the slots and other intricate shapes in the manufacturing industries. In the Milling of polymeric materials, several shortcomings observed during the process include fiber breakage, matrix decay, microcracking (Rajesh Mathivanan et al., 2016; Voss et al., 2017). However, the layer's influences can be affected during Milling because of its non-homogeneous structures such as delamination, fiber tearing, fibrous matrix interface, and thermal damage (Bagci & Yüncüoğlu, 2017). The most significant element concerning the surface quality of the machined component is finishing. In a machined surface, it occurs in the form of waviness (He et al., 2017). It creates measurement errors and reduced mechanical characteristics during the aerospace industry final assembly. The varying process constraints control is a precarious and time-consuming task while machining polymers. Its alteration can lead to several types of machining induced damages, as discussed in the prior art. It can be minimized through the control of parameters during the machining process. For this, various optimization modules exist in the literature. In contrast to the operating conditions, the tool geometry should be optimal to reduce defects. Most investigations were performed on the surface roughness, cutting tool geometry and cutting parameters (Ajith Arul Daniel et al., 2019; Ghafarizadeh et al., 2016; Hussain et al., 2016; Thakur & Singh, 2021). Ravi Sankar & Umamaheswarrao (2018) performed drilling operations of carbon/polymer composites. This works to estimate machining responses by employing Ant Colony Algorithm (ACO). The proposed ACO algorithm findings reveal that the objective function is significantly affected by the trailed and cutting velocity by cutting feed and depth. Vijayan and Rajmohan (2019) executed the drilling tests of CNT/CFRP hybrid composites by considering varying constraints. The hybrid approach optimizes the drilling characteristics such as thrust force, surface rough-

ness and delamination factor. The integrated module of the RSM and Swarm algorithm effectively provides the optimal parametric set. The hybrid approach finding reveals that increased feed rate raises the entry and exit delamination factors as well as thrust force, while drilling of the CNT/CFRP hybrid composites. The VIKOR is a multiple-criteria choice-making problem-solving method that resolves contradictory parameters by considering reasonable compromise. A closeness-based process evaluates the ideal proximity of the solution, and then it is utilized to assess the VIKOR index. Additionally, this technique is beneficial since it introduces three types of solutions that can be stated as a close-to-ideal, far-from-ideal and workable solution. The VIKOR technique has played a crucial role in resolving various engineering application issues involving multicriteria. Samson et al. (2020) have performed Abrasive water jet machining (AWJM) process on Inconel 718. They optimized the input constraints such as abrasive flow rate, standoff distance and jet-pressure to optimize the MRR, circularity, and taper angle using the VIKOR optimization technique. Furthermore, they concluded that 2 mm standoff distance, 180 MPa pressure and  $0.098^\circ$  taper provide a better hole quality and optimized value of MRR. Moreover, they also studied the surface structure of the machined surface. Sahu et al. (2020) has carried Electro discharge machining (EDM) on titanium alloy with the copper-tungsten-boron carbide tool. The authors have optimized the input parameters (viz., Percentage of boron and tungsten carbide, pulse-on-time, current, and duty cycle) of machining with the VIKOR method to maximize and minimize the Pareto solution obtained from multi-objective simple optimization algorithm for the MRR. Additionally, the algorithm easily applies to the process parameter with lesser computational effort. Chandrasekhar & Prasad (2020) have experimented with the micro-drilling behavior of metal matrix composite by Electrochemical machining (ECM). Authors optimize the different ECM operating parameters (i.e., electrolyte concentration, current, and voltage) with the Entropy-VIKOR technique to increase the metal removal rate and decrease the hole dilation and delamination of the composite machining. Furthermore, the machining set of 16 V voltage, 4 A current, and 3 mol of electrolyte concentration gives the optimized result of machining. Priti et al. (2021) perform the micro electrochemical discharge machining ( $\mu$ ECDM) process on carbon fiber laminates. The authors have studied different input parameters such as tool rotation, tool feed rate, and duty cycle. The MRR and overcut was optimized by the Entropy-VIKOR. The authors concluded that the Entropy-VIKOR method gives the most acceptable value with a minimum calculation. Moreover, the authors also examine the damaged surface of the machined hole with the optical micrograph. Krishnaraj et al. (Krishnaraj et al., 2012) evaluated various drilling parameters on the thin CFRP laminates to point out their impact on the laminate's structural integrity. The ideal cutting condition was attained by exploiting the Genetic algorithm (GA). Sait (2010)(Sait, 2010) applied two alternative evolutionary techniques to optimize process constraints during machining of GFRP pipe using GA and Swarm optimization. These algorithms were used to minimize the surface roughness, machining forces, and tool wear to achieve a singular optimal objective on specific optimum machining parameters. Researchers have recently used the TLBO algorithm to optimize manufacturing operations (Chate et al., 2019; Shadab et al., 2019). Abhishek, Rakesh Kumar, et al. (2017) performed the machining (Turning) experimentation of epoxy-based CFRP composites by the TLBO algorithm. The author utilized an HSS machining tool (Single-Point) for turning operation. In this study, Non-linear regression is first applied to determine objective functions based on various process parameters (angle of fiber orientation, spindle speed, depth of cut, and feed rate). A correlation analysis was performed on the nonlinear regressions to estimate the relationship between input factors and turning performances. This study explores metaheuristics computations to find the optimal parametric set. Kumar et al. (2020) have explored TLBO to optimize the EDM parameters. The authors stated that TLBO provides the optimal global solution for this multi optimization process parameter. Moreover, they also compared the TLBO algorithm with the three metaheuristic algorithm techniques to evaluate the module accuracy.

The findings of the extensive literature survey illustrated that ample work was conducted to endeavor and figure out the parametric combination by using evolutionary algorithms for a range of machining processes. But, a common disadvantage of GA, PSO, and SA algorithms is that they need to be calibrated. The calibration parameters must be optimized for the algorithms to perform appropriately. In contrast, optimum values of these calibration parameters are difficult to achieve, very critical for the algorithm's performance. Unlike other algorithms (GA, PSO, SA), TLBO is a population-based algorithm that imitates teaching-learning in any classroom. This technique does not need any precise algorithmic calibrating parameters. Another exciting aspect of the current work is the development of epoxy nanocomposites and parametric evaluation through a hybrid module of VIšekriterijumsko KOMPromisno Rangiranje (VIKOR) and TLBO. The production of CNO/polymer nanocomposite is significantly less explored in the existing database. Most of the studies focus on laminate and fiber composites. The composite research community has established many methods to evaluate the fiber-reinforced polymer (FRP) machining process. In earlier research, the scholars were generally concerned with the macro size fiber-reinforced polymer. This work is dedicated to CNO machining efficiency estimation. Also, the application of metaheuristic algorithms for machining analysis of epoxy nanocomposites is passing through the opening phase. It needs extra interest from the researcher society for the complete utilization of its improved properties. However, detailed studies on the Milling of CNO/polymer nanocomposite using the solid carbide tool with simultaneous response optimization are very limitedly explored in previous work.

The present work investigates an integrated and improved approach to appraise the varying constraints and estimation of CNO/polymer Milling efficiency. According to Box-Behnken Design (BBD), CNO filler content (A), cutting speed (B), feed rate (C) and depth of cut (D) are varied. The BBD-based Design of Experiment of 27 test array is utilized as an experimental layout, reducing the total number of experimental runs without losing the details related to process collection. Each variable was investigated for its effect on Milling characteristics such as Material Removal Rate and Surface roughness. VIKOR methodology transforms several metrics into a single output equivalent index called the assessment index. In order to find optimal machining conditions, a prominent metaheuristic approach such as TLBO is included in the proposed optimization

process. Milling is sophisticated machining as well as quality operation. Finally, the simultaneous optimization of all performance metrics is achieved through the proposed hybrid tool. An attempt has been made to overcome the existing optimization tool limitation by developing an efficient integrated module.

## 2. Experimental details

### 2.1 Sample preparation

The CNO/polymer nanocomposites samples are fabricated in two-phase. Initially, the CNO is dispersed into the acetone through the ultrasonication method for 45 minutes at 40 kHz to prevent agglomeration. Bisphenol A diglycidyl ether (BADGE) epoxy (Lapox L-12) is added to the mixture in the second step. The three varying weight percent concentration in the order of 0.5, 1.0, and 1.5 wt.% is used in the prepared mixture and again this mixture is sonicated for 45 minutes using a bath sonicator. The partial distillation process is used to separate the acetone from the mixture. Afterward, the hardener Triethylenetetramine (TETA, Lapox K-6) is added to the epoxy and mixed with the help of a magnetic stirrer. The ratio of 10:100 by weight of TETA to BADGE was taken, and then the mixture was poured into a metal mold of dimension (Fig. 1). The molds containing the mixture were kept for the whole day at ambient temperature for curing. Casted samples were taken out from the metallic molds(s) and left for a few hours for post-curing at room temperature.

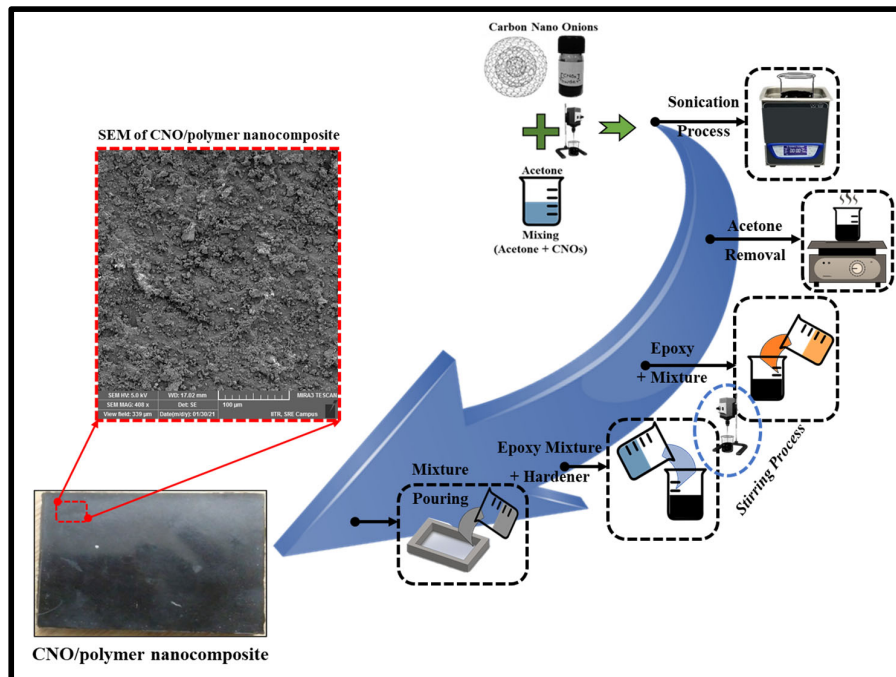


Fig. 1. Fabricated specimen of CNO/polymer nanocomposite for Milling tests

The four process controls, i.e., weight % of CNO filler content (A), cutting speed (B), feed rate (C) and depth of cut (D), were taken into account (Table 1). The Box-Behnken Design (BBD) based experimental array was utilized to carry out the Milling plan (Table 2). A solid carbide tool is used in the Milling test of the polymer nanocomposite. Each experimental run is done three times following the parametric setting depicted in Table 2 and images of the machined Milled slots are illustrated in Fig. 2 and Fig. 3.

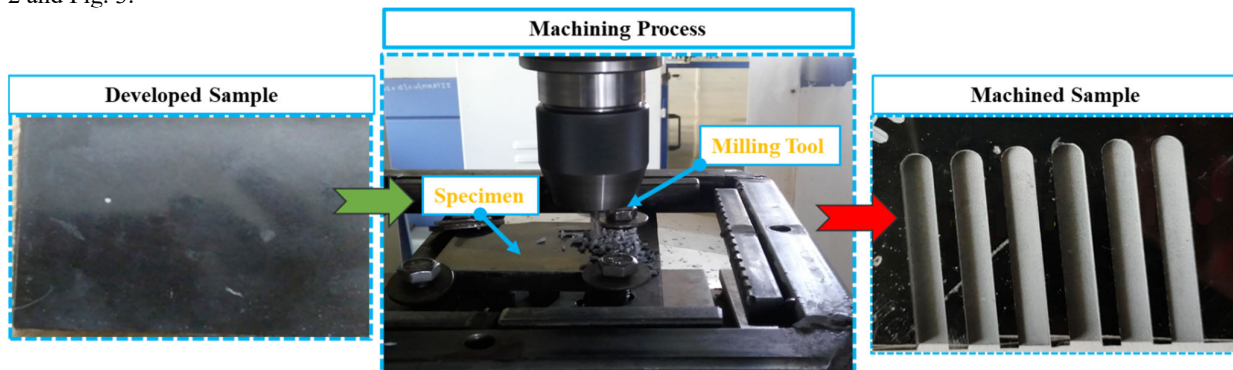
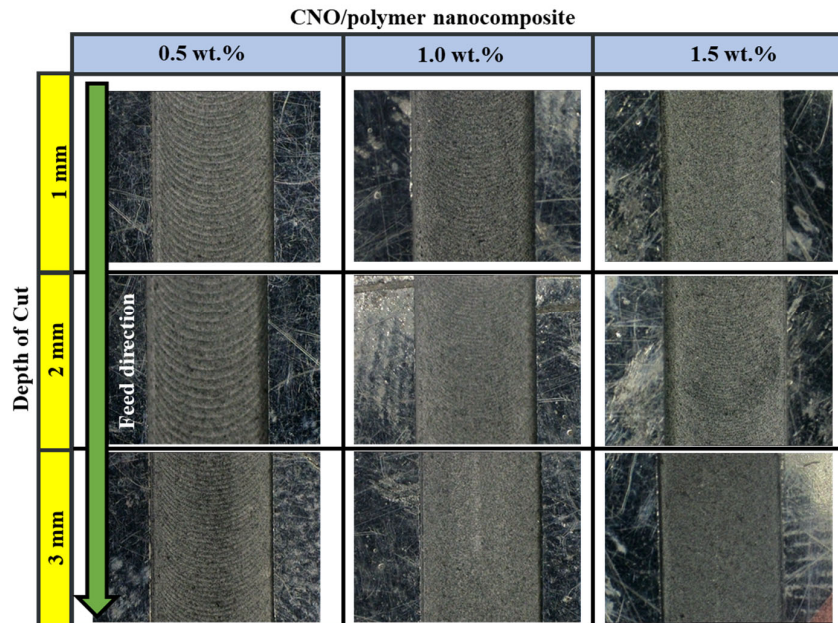


Fig. 2. Experimentation setup



**Fig. 3.** Machined samples (Milling slots)

**Table 1**

Process constraints

Levels	CNO Wt. %	Spindle Speed (rpm)	Feed rate (mm/min)	Depth of Cut (mm)
	<i>A</i>	<i>B</i>	<i>C</i>	<i>D</i>
1	0.5	500	50	1
2	1.0	1000	100	2
3	1.5	1500	150	3

**Table 2**

Experimental design and corresponding response value

Exp. No.	Process parameters				Process response	
	<i>A</i>	<i>B</i>	<i>C</i>	<i>D</i>	SR ( $\mu\text{m}$ )	MRR ( $\text{mm}^3/\text{min}$ )
1	0.5	500	100	1	3.428	9.059
2	1.5	500	100	2	3.396	11.180
3	0.5	1500	100	3	1.879	15.223
4	1.5	1500	100	1	1.780	7.479
5	1.0	1000	50	2	1.839	5.815
6	1.0	1000	150	3	3.153	22.569
7	1.0	1000	50	1	1.888	4.170
8	1.0	1000	150	2	2.688	17.049
9	0.5	1000	100	3	2.164	15.058
10	1.5	1000	100	2	2.095	11.303
11	0.5	1000	100	3	2.416	15.058
12	1.5	1000	100	1	1.979	7.400
13	1.0	500	50	2	2.179	5.752
14	1.0	1500	50	3	1.458	7.541
15	1.0	500	150	1	2.969	11.706
16	1.0	1500	150	2	2.220	17.237
17	0.5	1000	50	3	1.778	7.109
18	1.5	1000	50	1	1.880	4.521
19	0.5	1000	150	3	3.315	23.784
20	1.5	1000	150	1	2.452	12.297
21	1.0	500	100	2	3.440	11.762
22	1.0	1500	100	3	1.863	15.536
23	1.0	500	100	1	3.372	8.122
24	1.0	1500	100	2	1.883	12.019
25	1.0	1000	100	3	2.146	15.367
26	1.0	1000	100	1	2.031	8.211
27	1.0	1000	100	2	2.143	11.891

## 2.2 Milling responses

During end-milling experimentation, the slots were produced in the developed samples of CNO/polymer nanocomposite samples. To consistently measure the standard experimentation error, the central experiment was replicated three times, and the effects of each time were observed out of 27 sequences of experiments. As shown in Fig. 2 and Fig. 3, Milling experiments were performed with a width of 5 mm. The Milling operations were executed on a Vertical CNC Milling machine (Model: BMV/35 TC/20, Fig. 2). The cutting tool is the four-flute of 5 mm diameter finishing tool. The surface roughness (SR) was assessed using Surtronic S-128 as the portable surface roughness setup. For the observation MRR, Eq. (1) is utilized for the computation.

$$MRR = \frac{\text{Specimen weight}_{\text{initial}} - \text{Specimen weight}_{\text{Final}}}{\text{Time of machining } (t_m) \times \text{Density}(\rho)} \text{ (mm}^3/\text{min)} \quad (1)$$

## 3. Methodology

### 3.1 Višekriterijumsko KOmpromisno Rangiranje (VIKOR) methodology

VIKOR is a strategy for ranking alternative solutions and decides to select the various criteria (Opricovic & Tzeng, 2007). A Multi-response optimization problem may be executed by making use of this approach. According to the characteristics of the solutions, VIKOR solves the problem of multi-response optimization, then normalizes the outputs between 0 and 1 (Ebrahimnejad et al., 2012). The VIKOR approach employs a technique that is outlined as follows.

**Step 1:** Estimation of the specific normalized value ( $d_i$ ) for each response ( $\hat{y}_j$ ):

Larger-the-better (LTB)

$$d_i = \begin{cases} 1 & , \hat{y}_j < \hat{y}_{\min} \\ \left( \frac{\hat{y}_j - \hat{y}_{\min}}{\hat{y}_{\max} - \hat{y}_{\min}} \right)^t & , \hat{y}_{\min} < \hat{y}_j < \hat{y}_{\max}, t \geq 0 \\ 0 & , \hat{y}_j \geq \hat{y}_{\max} \end{cases} \quad (2)$$

Smaller-the-better (STB)

$$d_i = \begin{cases} 1 & , \hat{y}_j < \hat{y}_{\min} \\ \left( \frac{\hat{y}_j - \hat{y}_{\max}}{\hat{y}_{\max} - \hat{y}_{\min}} \right)^t & , \hat{y}_{\min} < \hat{y}_j < \hat{y}_{\max}, t \geq 0 \\ 0 & , \hat{y}_j \geq \hat{y}_{\max} \end{cases} \quad (3)$$

where  $\hat{y}_j$  = Observed experiential value,  $\hat{y}_{\max}$  = highest experiential value,  $\hat{y}_{\min}$  = lowest experiential value, and Exponent 't' represents the degree of significance in acquiring the objective value.

**Step 2:** Compute Utility ( $\bar{S}_i$ ) and Regret ( $\bar{R}_i$ ) measures of each experiment.

$$\bar{S}_i[d_i] = \sum \frac{w_j(a_{ij}^{\max} - d_j^*)}{d_{ij}^{\max} - d_{ij}^{\min}} \quad (4)$$

$$\bar{R}_i[d_i] = \text{Max}_j \frac{w_j(a_{ij}^{\max} - d_j^*)}{d_{ij}^{\max} - d_{ij}^{\min}} \quad (5)$$

where  $w_j$  = represents weightage provided to individual responses  $\sum w_i = 1$ . whose value is considered as 0.5 to guarantee an impartial assessment of all machining responses.

**Step 3:** Determination of VIKOR assessment index for the  $i^{\text{th}}$  experiment.

$$V_i = \vartheta \left( \frac{\bar{S}_i - \bar{S}^{\min}}{\bar{S}^{\max} - \bar{S}^{\min}} \right) + (1 - \vartheta) \left( \frac{\bar{R}_i - \bar{R}^{\min}}{\bar{R}^{\max} - \bar{R}^{\min}} \right) \quad (6)$$

where,  $i = 1, 2, 3, \dots, n$  and

$\bar{S}^{\min} = \text{Min of } \bar{S}_i, \bar{S}^{\max} = \text{Max of } \bar{S}_i$

$\bar{R}^{\min} = \text{Min of } \bar{R}_i, \bar{R}^{\max} = \text{Max of } \bar{R}_i$

$\vartheta$  illustrates the weight for taken maximum group utility, it is typically defined as 0.5.

**Step 4:** ANOVA performance to identify various parameter contributions to the desired response and conduct a validation test.

### 3.2 Teaching Learning Based Optimisation (TLBO) algorithm

TLBO term stands for the “Teaching learning-based optimization” procedure, parted into two phases; the first phase is known as the Teachers and the second phase is known as the Learners Phase. The definition of classism is used in most of the swarm intelligence and evolutionary algorithms that have been used over time. Each batch of the worst responses is replaced by superior (Chau et al., 2018; Shadab et al., 2019; Sharma et al., 2020). While using the TLBO algorithm, after swapping the worst responses with best responses only after the learner process, repeated explanations need to be changed to prevent freezing into the optimal local value if replicated solutions are observed. Rao et al. (2011) research demonstrates that repeated solutions were changed by modifying arbitrarily opted parameters before the next-generation execution. Besides, the impact of typical algorithm operating conditions, i.e., population size, number of iterations, and best fitness value, on algorithm output was also explored by evaluating different controlling parameters (Rao & Patel, 2012).

The TLBO procedure has described the two essential types of the learning process:

1. The Teacher or Tutor is called the **Teacher phase**.
2. By the communication, along with the additional students called the **Learner phase**.

Basically, the "TLBO" concisely defined as a function optimization method as well as the "Orthogonal design" give specific properties of the orthogonal design technique.

#### 3.2.1 Teacher phase

Teachers are generally considered to be highly skilled in a grouping, and at this stage, teachers share their expertise with all learners. A qualified teacher can get his/her students to their level of understanding. However, it is not realistic, and a teacher can only raise the means of the group of learners  $C_1$  to some improved value  $C_2$ , which depends on the learner's capacity and can be better than  $C_1$ .

Considered that  $C_j$  is mean and  $L_j$  is the teacher at every iteration value, i.e.,  $j$ .  $L_j$  will now strive to improve the mean  $C_k$  to it so that the new mean is  $L_j$  as  $C_{new}$ , and the difference between the previous mean and the latest mean is given by:

$$d\_m_j = rd_j(C_{new} - f_T C_k) \quad (7)$$

Where  $d\_m_j$  is the difference of means,  $f_T$  depicts the factor of teaching which chooses the average score also to be modified, and  $rd_j$  represents a random number in between 0 and 1.  $f_T$  can either be 1 or 2, which is an algorithmic measure and is randomly determined with following probabilistic equation:

$$f_T = \text{round} [1 + \text{rand}(0,1)\{2 - 1\}] \quad (8)$$

Therefore, such disparity alters the current solution in the following equation:

$$X_{new,j} = X_{old,j} + d\_m_j \quad (9)$$

#### 3.2.2 Learner phase

Interaction between the learners and teachers has contributed to an improvement of their awareness in this process. If a learner has more experience of inherited knowledge than the other learner, then their expertise would be improved. This stage's learning process is illustrated as follows, considering the population size value to be  $n$ .

At any iteration  $j$ , considering two different learners  $X_j$  and  $X_k$  where  $j \neq k$

$$X_{new,j} = X_{old,j} + rd_j(X_j - X_k) \quad \text{if } f(X_j) < f(X_k) \quad (10)$$

$$X_{new,j} = X_{old,j} + rd_j(X_k - X_j) \quad \text{if } f(X_j) > f(X_k) \quad (11)$$

Consider  $X_{new}$  if it gives an improved fitness function value.

The detailed methodology in the form of the TLBO flow chart is explained in Fig.4.

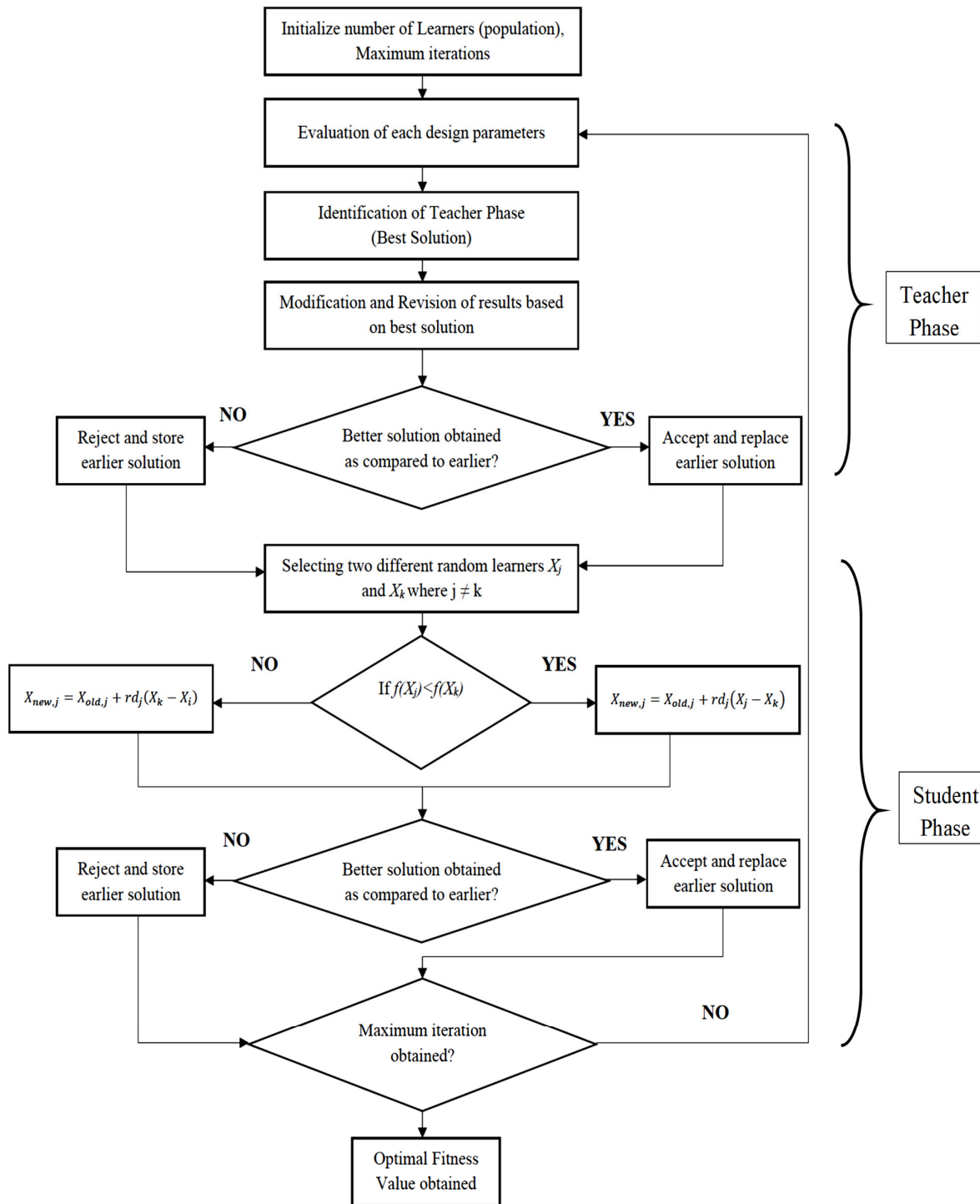


Fig.4. TLBO Flow-Chart (R. V. Rao et al., 2011)

### 3.3 VIKOR-TLBO hybrid module

This study utilizes RSM modeling to establish a correlation between varying constraints and Milling responses. The response in this model is approximated using the First order equation, as shown below;

$$y = \alpha_0 + \sum_{i=1}^n \alpha_i X_i + e \quad (12)$$



where  $i, j = 1, 2, 3, \dots, n$ ,  $\alpha_0$ ,  $\alpha_i$ , and  $\alpha_{ij}$  are the coefficients in the mathematical model,  $X_i$  and  $X_{ij}$  is the variable process parameters, and  $e$  is the obtained modeled experimental error. Subsequently, TLBO is used as an evolutionary algorithm to resolve the optimization problems achieved by means of experimentation. The structure of the VIKOR-TLBO hybrid module is shown in Fig.5. This work aims to reduce the surface roughness and improve machining productivity (MRR). VIKOR technique is employed to aggregate the multiple responses during the Milling experimentations. VIKOR converts the process responses into a single objective function used as a fitness function in the TLBO algorithm.

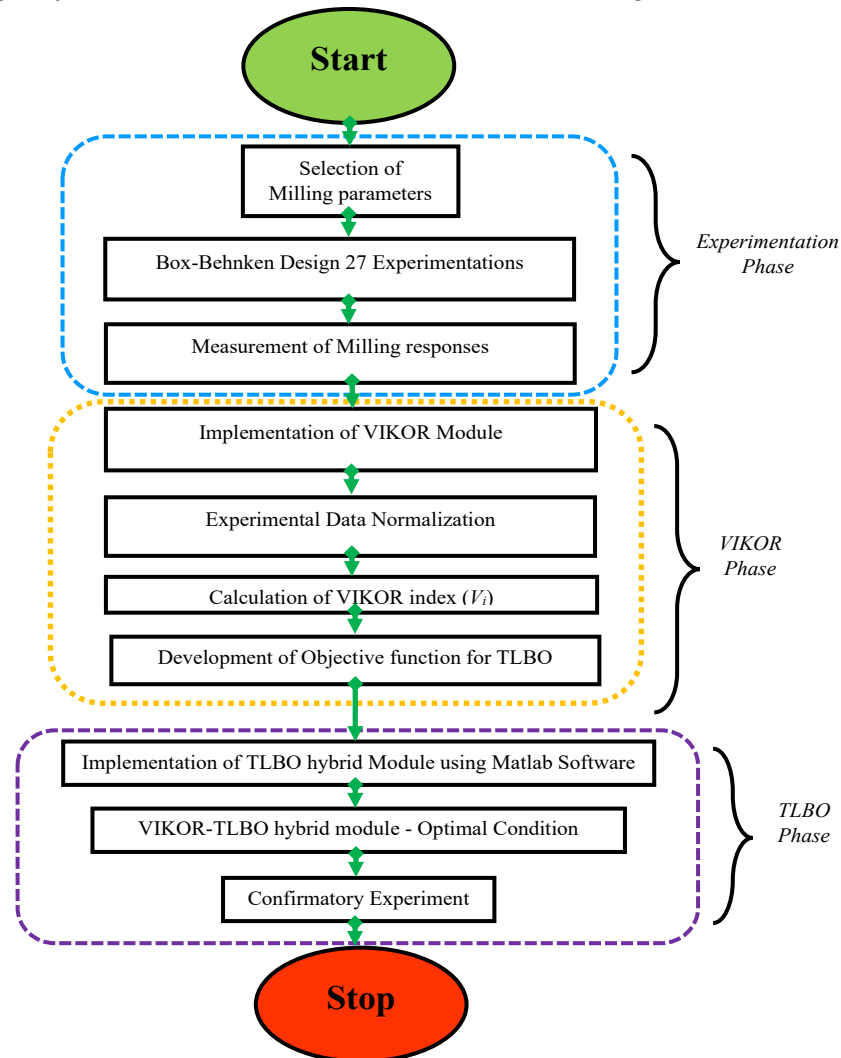


Fig. 5. Flowchart for VIKOR-TLBO hybrid module

#### 4. Results and Discussion

The tests were primarily designed to comply with the Box-Behnken Design 27 experimentations. Table 2 shows the design array for process parameters and Milling responses. Consequently, a possible compromise has been set up by utilizing the hybrid VIKOR based metaheuristic TLBO algorithm.

##### 4.1 ANOVA for Milling responses

ANOVA is the variance calculation of the data observed from SR and MRR using statistical analysis software (Table 3). It is noted that the spindle speed and feed rate are the most significant factors for both responses. Additionally, the most critical machining factor for SR is spindle speed and feed rate, as per the statistical analysis. Similarly, for MRR, the most influencing factors are feed rate and depth of cut.

According to the defined machining variables, the BBD 27 based regression model for SR and MRR can be considered as:

$$SR = 2.760 - 0.149 \times A - 0.001336 \times B + 0.00963 \times C + 0.0633 \times D \quad (13)$$

$$MRR = -6.28 - 0.616 \times A + 0.000053 \times B + 0.11622 \times C + 3.427 \times D \quad (14)$$

For SR and MRR,  $R^2$  reveals that the % error of the developed regression equation as the proportion of overall error is 80.39% and 94.54%, respectively. Similarly, adjusted error as a proportion of the total error  $R^2$ - adj. is 76.80% and 93.55%, respectively, which reveal that the established regression model is significant and can be considered to navigate the design space (Babu et al., 2019; Jenarthan et al., 2016).

**Table 3**  
ANOVA for machining responses

Source	DF	Seq SS	Contribution	Adj SS	Adj MS	F-Value	P-Value	Remark
Surface roughness (SR)								
<b>Model</b>	4	7.92593	80.39%	7.92593	1.98148	22.54	0.000	Significant
<b>Linear</b>	4	7.92593	80.39%	7.92593	1.98148	22.54	0.000	Significant
<b>A</b>	1	0.16318	1.66%	0.04419	0.04419	0.50	0.486	Not Significant
<b>B</b>	1	4.94016	50.10%	4.47387	4.47387	50.89	0.000	Significant
<b>C</b>	1	2.78020	28.20%	2.78020	2.78020	31.63	0.000	Significant
<b>D</b>	1	0.04239	0.43%	0.04239	0.04239	0.48	0.495	Not Significant
<b>Error</b>	22	1.93398	19.61%	1.93398	0.08791			
<b>Lack-of-Fit</b>	21	1.90229	19.29%	1.90229	0.09059	2.86	0.439	
<b>Total</b>	26	9.85991	100.00%					
Material Removal Rate (MRR)								
<b>Model</b>	4	635.571	94.54%	635.571	158.893	95.27	0.000	Significant
<b>Linear</b>	4	635.571	94.54%	635.571	158.893	95.27	0.000	Significant
<b>A</b>	1	80.656	12.00%	0.757	0.757	0.45	0.508	Not Significant
<b>B</b>	1	25.386	3.78%	0.007	0.007	0.00	0.949	Not Significant
<b>C</b>	1	405.244	60.28%	405.244	405.244	242.97	0.000	Significant
<b>D</b>	1	124.284	18.49%	124.284	124.284	74.52	0.000	Significant
<b>Error</b>	22	36.693	5.46%	36.693	1.668			
<b>Lack-of-Fit</b>	21	36.693	5.46%	36.693	1.747			
<b>Total</b>	26	672.263	100.00%					

4.2 Impact of Milling constraints on machining performances

The statistical models have examined the effect of process variables on Milling responses. Fig.6 and 7 illustrate that Surface roughness (SR) lowers with CNO inclusion to the matrix material, owing to the disparity in the epoxy matrix. It decreases substantially with the addition of nano reinforcement (Harii Krishna Rao et al., 2012; D. Kumar & Singh, 2016). It is feasible due to the self-lubricating behavior of reinforced nanomaterials; the value of SR decreases proportionally with decreasing speed from 500 rpm to 1500 rpm (Ali et al., 2019). It is further obtained that, with a higher feed rate, the SR increases as a result of the occurrence of strain hardening effect in CNO/ polymer nanocomposite during machining (Akinlabi et al., 2018). SR is improved as the depth of cut increases due to large material removal from the surface, resulting in the Milled specimen rougher surface(Thakur & Singh, 2021).

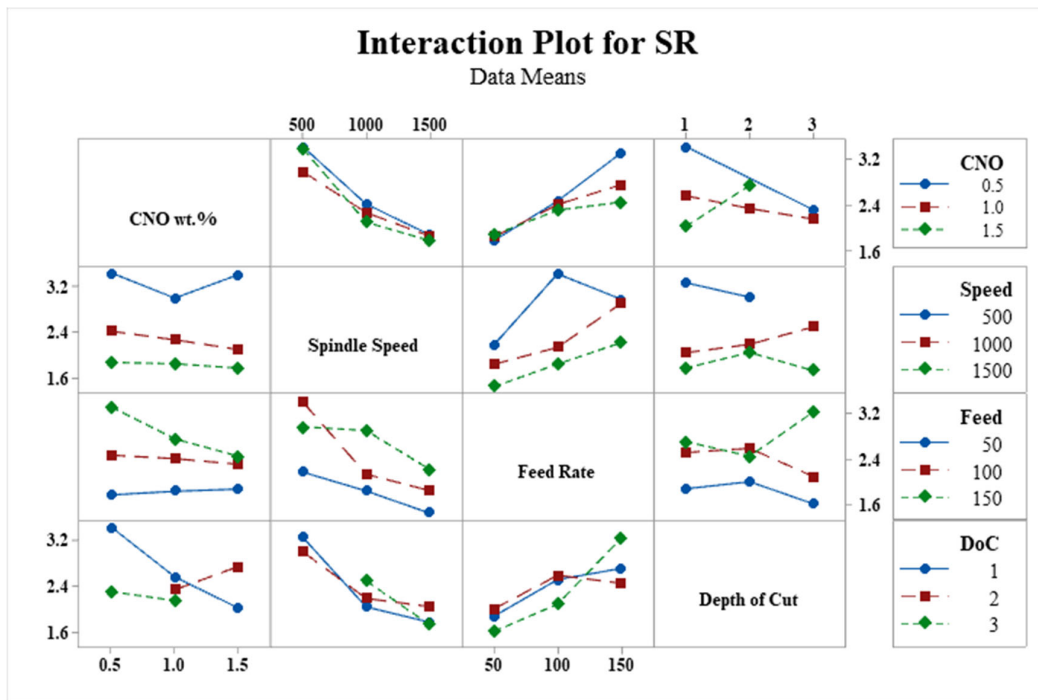


Fig. 6. Interaction Plot for Surface roughness (SR)

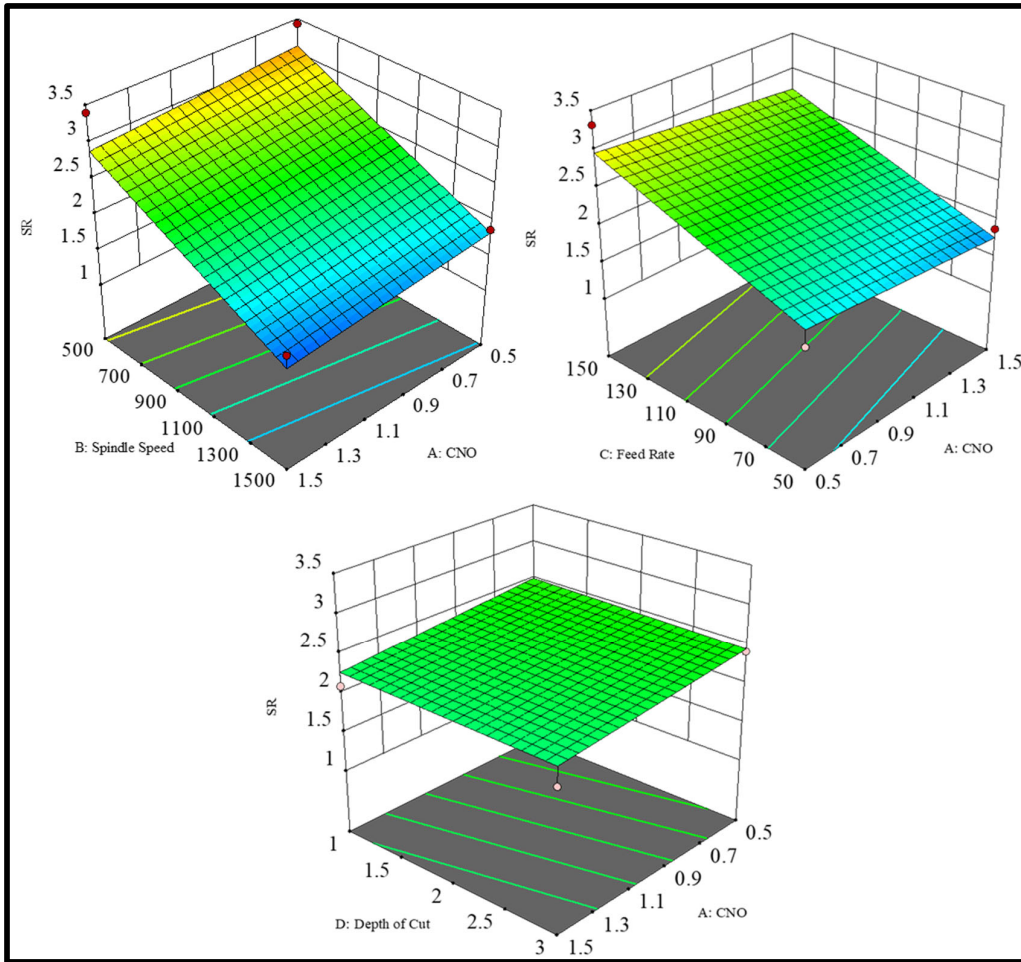


Fig. 7. 3D Plot for Surface roughness (SR)

From Fig.8 and 9, It has been observed that the MRR decreases with rising CNO inclusion. At higher wt.% of CNO, the rate of MRR decreases, which increases the machinability of the epoxy matrix (Paulo Davim et al., 2009). As a result, the removal of fine particulates during Milling experimentation is improved. Furthermore, the performance of MRR enhanced in a meaningful manner with a raise in spindle speed (B), feed rate (C), and depth of cut (D) since higher cutting depth is accounted for larger chip thickness and increased feed rate refers to tool displacement into the material (Cha et al., 2019).

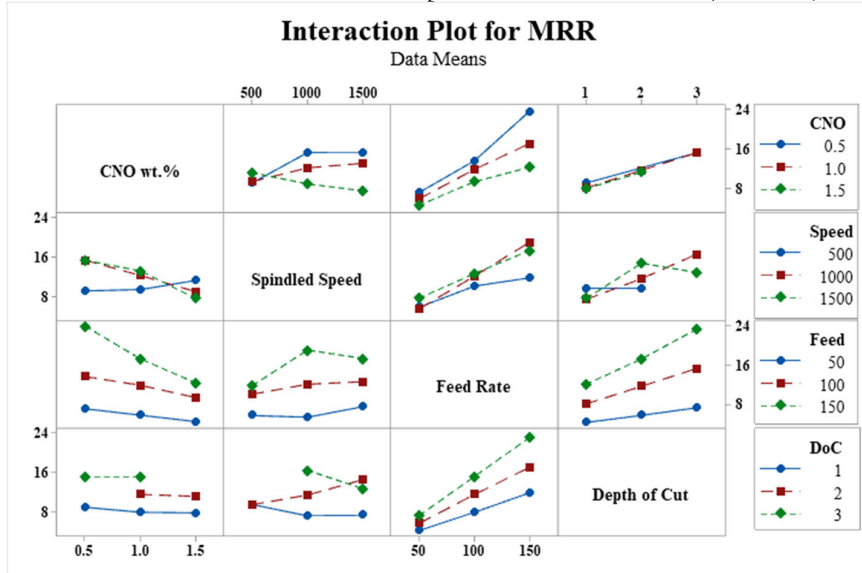


Fig. 8. Interaction Plot for MRR

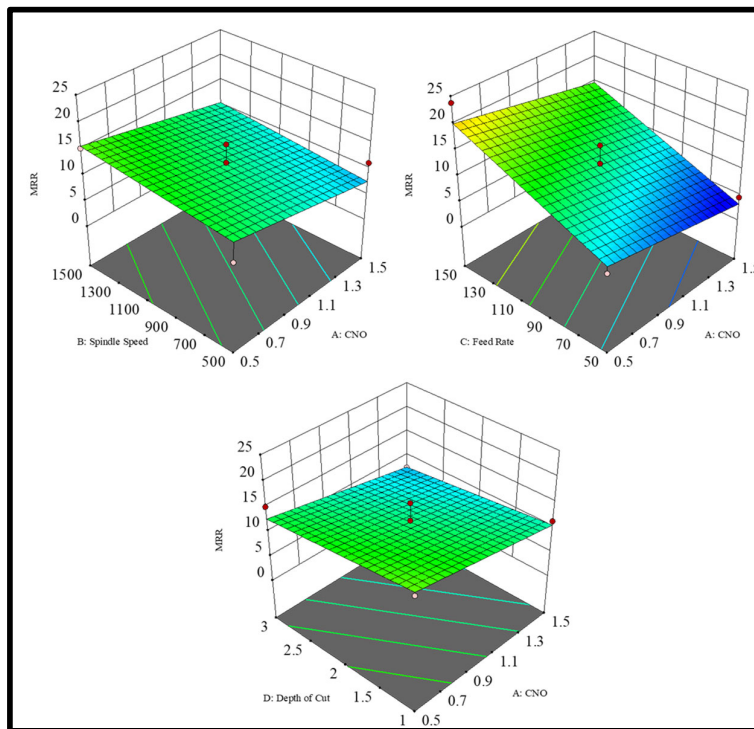


Fig. 9. 3D Plot for MRR

### 4.3 VIKOR methodology

In the end-milling procedure, multi-response is generally contradictory in its characteristics. The factors affect each measure of performance in diverse ways. There is always a different percentage influence of all process constraints on the machinability measures. Surface roughness (SR) needs to be minimized, whereas Material Removal Rate (MRR) must be maximized to obtain the best optimal output from end-milling machining. Multi-response optimization strategies are typically used to pick different process parameters correctly. The deviation sequence is formed by Eqs. (2-3) for each response, and the deviation sequence is determined. Finally, the VIKOR index ( $V_i$ ) is determined using Eq. (6), as shown in Table 4.

**Table 4**  
Calculation of VIKOR index ( $V_i$ )

Exp No.	Unity and Regret Value Measurement		VIKOR index ( $V_i$ )	Rank
	$\bar{S}_i$	$\bar{R}_i$		
1	0.128	0.125	0.038	26
2	0.190	0.179	0.161	25
3	0.675	0.394	0.856	4
4	0.503	0.419	0.736	8
5	0.446	0.404	0.668	12
6	0.541	0.469	0.833	5
7	0.391	0.391	0.604	19
8	0.518	0.328	0.636	15
9	0.599	0.322	0.699	11
10	0.521	0.339	0.653	13
11	0.536	0.278	0.588	20
12	0.451	0.369	0.628	16
13	0.358	0.318	0.483	21
14	<b>0.586</b>	<b>0.500</b>	<b>0.911</b>	<b>1</b>
15	0.311	0.192	0.284	23
16	0.641	0.333	0.750	7
17	0.494	0.419	0.729	9
18	0.402	0.394	0.616	18
19	0.532	0.500	0.863	3
20	0.456	0.249	0.483	22
21	0.194	0.194	0.183	24
22	0.688	0.398	0.872	2
23	0.118	0.101	0.000	27
24	0.593	0.393	0.783	6
25	0.612	0.326	0.716	10
26	0.458	0.355	0.618	17
27	0.524	0.327	0.640	14

For further calculation, the distinguishing coefficient weight is considered to be 0.50 into account in calculating the  $V_i$ . In Table 4, based on the VIKOR index, the experiments were ranked. It is noticed that experiment no.14 acquired the highest value as 0.911, which agrees to the optimal set amongst executed experiments corresponding to Box-Behnken Design 27 experimentations A2-B3-C1-D3, i.e., 1 wt.% CNO, 1500 rpm spindle speed, 50mm/min feed rate, and depth of cut value equals to 3 mm. In contrast, the result obtained by the RSM-based optimizer for SR and MRR is obtained as A3-B3-C1-D3, i.e., 1.5 wt.% CNO, 1500 rpm spindle speed, 50mm/min feed rate, and depth of cut value equals to 3 mm (Fig. 10). The ANOVA reveals that the most critical factors affecting Milling characteristics are feed rate and weight % of CNO. The proper control of both the factor is highly required for efficient machining responses.

#### 5.4 The hybrid module of VIKOR and TLBO algorithm (VIKOR-TLBO)

A statistical variance analysis (ANOVA) is performed to estimate the importance of input parameters and their influence on the output function. The confidence level for the ANOVA is taken to be 0.95 for evaluation. In ANOVA, if a value less than 0.05 for an input parameter is estimated to be the  $P$ -value (probability), the particular parameter would significantly affect the performance measures. ANOVA is evaluated for the machining factors and continuous responses. With the contribution of 71.16% and 7.71% for spindle speed and cutting depth obtained, respectively, from ANOVA (illustrated in Table 5). The greater value of the determination coefficient describes the fitness of the model. This article utilizes a linear regression model to construct a statistical module. The regression equation for the VIKOR index ( $V_i$ ) with an  $R^2$  value of 80.25%, shown as:

$$VIKOR = -0.197 + 0.0635 \times A + 0.000535 \times B - 0.000271 \times C + 0.1098 \times D \quad (15)$$

The above equation is fed in the TLBO algorithm as an objective function. The optimal parametric function is achieved by running the TLBO algorithm in MATLAB software. A comparable clarification was undertaken by (Abhishek, Kumar, et al., 2017) during multicriteria optimization. The algorithm searches the optimal condition of varying initialization constraints.

**Table 5**

ANOVA for VIKOR index ( $V_i$ )

Source	DF	Seq SS	Contribution	Adj SS	Adj MS	F-Value	P-Value	Remark
<b>Model</b>	4	1.32783	80.25%	1.32783	0.331958	22.35	0.000	Significant
<b>Linear</b>	4	1.32783	80.25%	1.32783	0.331958	22.35	0.000	Significant
<b>A</b>	1	0.02063	1.25%	0.00804	0.008036	0.54	0.470	Not Significant
<b>B</b>	1	1.17740	71.16%	0.71736	0.717363	48.31	0.000	Significant
<b>C</b>	1	0.00220	0.13%	0.00220	0.002198	0.15	0.704	Not Significant
<b>D</b>	1	0.12760	7.71%	0.12760	0.127600	8.59	0.008	Significant
<b>Error</b>	22	0.32670	19.75%	0.32670	0.014850			
<b>Lack-of-Fit</b>	21	0.32053	19.37%	0.32053	0.015263	2.47	0.468	
<b>Total</b>	26	1.65453	100.00%					

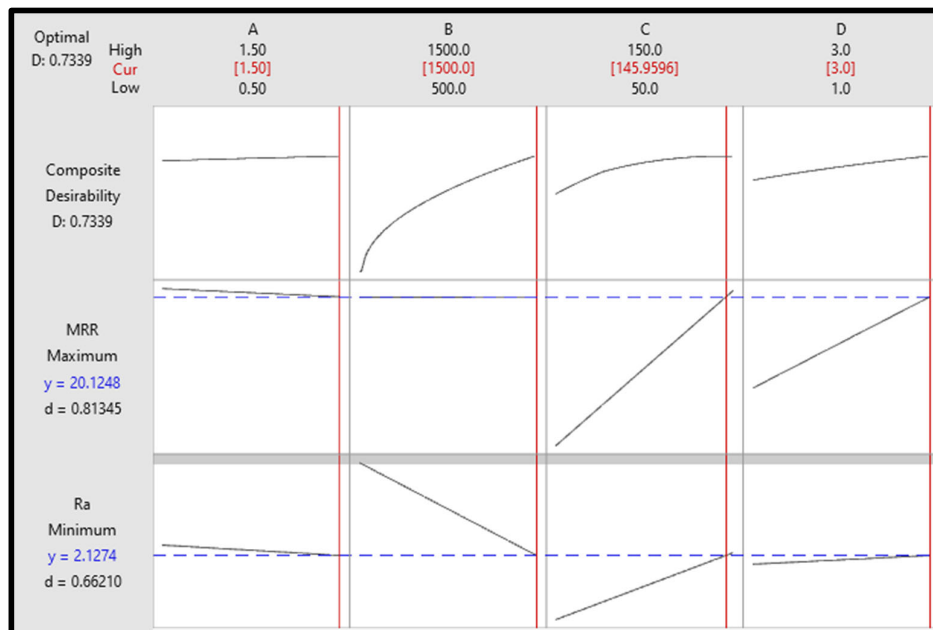


**Fig.10.** Optimal setting by Box-Behnken Design

Fig.11 demonstrates the TLBO algorithm convergence plot, obtained at the 0.940 optimal fitness function value. This value resembles the optimal constraints condition as A3-B3-C1-D3, i.e., 1.5 wt.% CNO, Spindle Speed at 1500 rpm, Feed at 50mm/min and 3 mm of cutting depth. The higher value of CNO weight percentage in the TLBO algorithm suggests the better value of SR while Milling experimentation of CNO/ polymer nanocomposite. Furthermore, the MRR obtained to be higher zone, which impacts more significantly on Milling performance.

### 5.5 Validation Test

A comparative test is illustrated in Table 7 between prediction obtained and priorly proven evolutionary meta-heuristic algorithms. The VIKOR coupled TLBO algorithm convergence plot is represented in Fig.11. It is reflected that the overall optimal value evaluated by the VIKOR methodology significantly improved the objective function value of 0.911 to 0.940 in the case of the TLBO algorithm-based optimization. To verify the optimal settings and solution achieved *via* VIKOR-TLBO, these results have also been validated with that obtained by three GRA modified metaheuristic algorithms *viz.* GA and SA (Simulated Annealing algorithm); there has been a good agreement observed between these results (depicted in Fig. 12). Table 6 signifies the values of specific algorithmic parameters for TLBO, GA and SA.

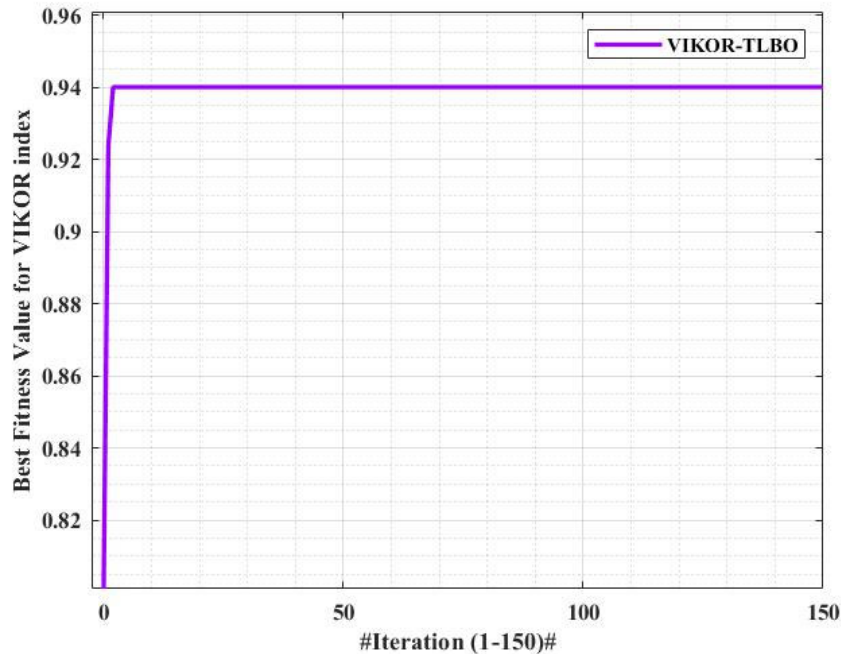


Fig. 11. Convergence plot of VIKOR-TLBO hybrid module

Table 6

Algorithm's constraints

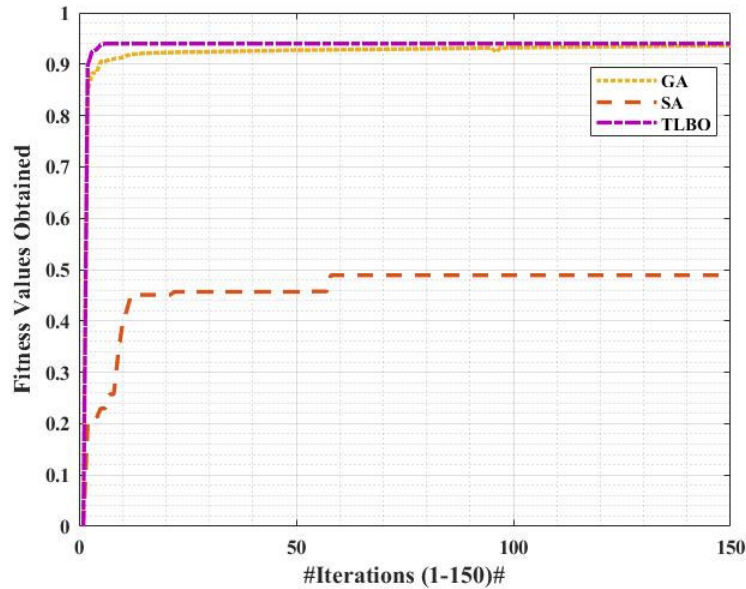
Metaheuristic Method	Parametric Setting
TLBO	Variables = 4 Population size = 30 Iterations = 150
GA	Variables = 4 Crossover function = Heuristic Crossover rate = 0.8 Selection function = Roulette wheel Mutation function = Adaptive feasible Scaling function = Rank Population size = 30 Iterations = 150
SA	Initial setting = [0.5 500 50 1] Initial temperature = 100°C Category = Boltzmann annealing Iterations = 150

**Table 7**

Comparative evaluation of evolutionary algorithms

Methods	Optimal Parametric Setting	Objective function Value	Observation*
VIKOR	A2   B3   C1   D3	0.911	Feasible
VIKOR-TLBO	A3   B3   C1   D3	0.940	Highly Feasible
VIKOR-GA	A3   B3   C1   D3	0.918	Moderately Feasible
VIKOR-SA	A3   B1   C1   D3	0.484	Less Feasible

\* VIKOR value is used as fixed point of reference, for comparison purposes.

**Fig. 12.** Comparison of Fitness function of GA, PSO and TLBO

The confirmatory test was performed to validate the outcomes of the proposed machining approach. The findings of the confirmatory test are illustrated in Table 8 between prediction and experimental observations. It can be noted that the predictive error of the VIKOR-TLBO algorithm optimum for the SR and MRR are 1.177 and 1.070%, respectively.

**Table 8**

Confirmatory Test

Responses	Experimental Values	VIKOR-TLBO Predicted	Error %
SR ( $\mu\text{m}$ )	1.189	1.203	1.177
MRR ( $\text{mm}^3/\text{min}$ )	8.872	8.967	1.070

$$\text{Improvement \%} = \frac{|\text{Predicted Values} - \text{Experimental Values}|}{\text{Experimental Values}} \times 100$$

### 5.5.1 Microscopic assessment of experimental and predicted machined surface

The machined sample was observed with a microscope image at experimental and predicted cutting conditions to demonstrate the composite interfaces micro deterioration at different Milling operation levels, illustrated in Fig. 13. With reference to Fig. 13(a), the image shows deeper feed marks, cavity holes, and crack occurred at the slot region on 1.0 % CNO/polymer nano-composite specimen. It is mainly due to the effect of the resin (Yang et al., 2020). Also, it is softened with the increase of cutting temperature and nanomaterials accumulation; therefore, the surface finish is less as compared to Fig. 13(b). The deeper feed markings impact surface quality and the machined surface is susceptible to deterioration (Buchholz et al., 2012). The mutual effect of CNO weight percent and parametric constraint is shown in Figs. 6 and 8 for SR and MRR, respectively, which have the lubricating property of CNO and the softness property of epoxy matrix material. It is achievable because a higher weight percentage of CNO nanofiller reduces friction coefficient during polymer machining (Fu et al., 2020). Because of the lower friction, less heat was created between the machine and tool interface, resulting in excellent surface quality (Dhiraj Kumar & Gururaja, 2020).

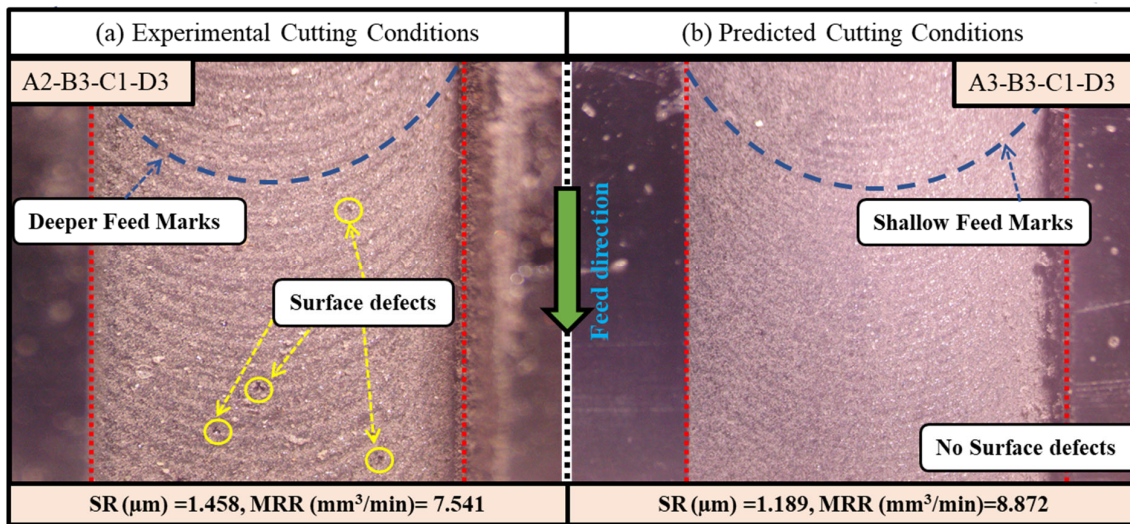


Fig. 13. Microscopic view of the Milling slot (machined surface)

## 5. Conclusion

This article focuses on the development of CNO/polymer nanocomposites and the effect of Milling constraints on the Material Removal Rate (MRR) and Surface roughness (SR). A multi-criterion decision-making methodology modified by a metaheuristic technique (TLBO) is used to select process variables. This module effectively provides an optimal solution for the superior MRR and minimal SR during machining. The following conclusion can be drawn based on the obtained findings:

- The hybrid module of VIKOR-TLBO successively aggregated the multiple responses during the Milling test. The experiment results show that increment in MRR and reduction in SR during Milling operation of CNO/polymer nanocomposite up to a threshold limit, having feed rate has the most critical factor for influencing the machining attributes.
- ANOVA identifies the essential process parameters for machining response. ANOVA results illustrate that the Surface roughness (SR) affirmed that the spindle speed (B) has the uppermost percentage contribution of 50.10% on the process parameters. Whereas Material Removal Rate (MRR) observed that spindle speed (B) has the highest percentage contribution (60.28%), and depth of cut (D) has the second-highest percentage contribution (18.49%).
- The linear regression equation developed for observational data shows a significant correlation between the empirical and the estimated value. The convergence plot results confirmed the potential significance of the Modified TLBO convergence rate in deciding the desired result.
- The optimal condition was evaluated based on VIKOR-TLBO values. Accordingly, the process parameters of CNO wt% - 1.5, Spindle Speed – 1500 rpm, Feed rate - 50 mm/min, and Depth of Cut – 3mm were observed to yield the anticipated findings.
- The higher value of depth of cut is observed in the case of the modified TLBO algorithm, which implies the effect of higher cutting speed in the course of Milling experimentation of CNO/polymer nanocomposite. The combination of higher feed rate and depth of cut impacts the materials in close interaction with the edge and gradually improves SR and MRR.
- The value obtained from the VIKOR-TLBO is 0.940, and the confirmatory experimental value is 0.911, which indicates the superior prediction performance of modified TLBO with a 3.183% error.

Consequently, the current study developed a robust hybrid module of VIKOR-TLBO for multicriteria optimization. It can be customized to a broad range of functional research-related challenges for any number of variable characteristics. In addition to encouraging production precision, this predictive approach might be used for other traditional (drilling, grinding, turning, etc.) and non-conventional (ECDM, WJM, EDM, etc.) manufacturing operations for CNO modified polymer composites. The higher application potential of VIKOR-TLBO based hybrid modules can be used for case studies of industrial engineering and commercial surveys having varying constraints. The higher utility of the CNO/polymer nanocomposite material described the feasibility of multifunctions. Future investigations on CNO polymers machining performances such as tool wear, tooltip temperature, machining defects, matrix failures, chip formation, and chip shapes could be explored for efficient machinability computations.



## Acknowledgment

The authors would like to acknowledge the Council of Science and Technology, Lucknow, India.

## Declaration of Conflicting Interests

The authors declared no potential conflicts of interest.

## Funding

This work is financially sponsored by the Uttar Pradesh Council of Science and Technology, Lucknow, India, under the research project scheme [R&D project ID-UPCST/ D-2491].

## References

- Abhishek, K., Kumar, V. R., Datta, S., & Mahapatra, S. S. (2017). Application of JAYA algorithm for the optimization of machining performance characteristics during the turning of CFRP (epoxy) composites: comparison with TLBO, GA, and ICA. *Engineering with Computers*, 33(3), 457–475. <https://doi.org/10.1007/s00366-016-0484-8>
- Abhishek, K., Rakesh Kumar, V., Datta, S., & Mahapatra, S. S. (2017). Parametric appraisal and optimization in machining of CFRP composites by using TLBO (teaching–learning based optimization algorithm). *Journal of Intelligent Manufacturing*, 28(8), 1769–1785. <https://doi.org/10.1007/s10845-015-1050-8>
- Agrawal, S., Singh, K. K., & Sarkar, P. (2014). Impact damage on fibre-reinforced polymer matrix composite – A review. *Journal of Composite Materials*, 48(3), 317–332. <https://doi.org/10.1177/0021998312472217>
- Ajith Arul Daniel, S., Pugazhenthii, R., Kumar, R., & Vijayananth, S. (2019). Multi objective prediction and optimization of control parameters in the milling of aluminium hybrid metal matrix composites using ANN and Taguchi -grey relational analysis. *Defence Technology*, 15(4), 545–556. <https://doi.org/10.1016/j.dt.2019.01.001>
- Akinlabi, E. T., Mathoho, I., Mubiayi, M. P., Mbohwa, C., & Makhatha, M. E. (2018). Effect of process parameters on surface roughness during dry and flood milling of Ti-6Al-4V. *2018 IEEE 9th International Conference on Mechanical and Intelligent Manufacturing Technologies (ICMIMT), 2018-Janua*, 144–147. <https://doi.org/10.1109/ICMIMT.2018.8340438>
- Ali, I., Basheer, A. A., Kucherova, A., Memetov, N., Pasko, T., Ovchinnikov, K., Pershin, V., Kuznetsov, D., Galunin, E., Grachev, V., & Tkachev, A. (2019). Advances in carbon nanomaterials as lubricants modifiers. *Journal of Molecular Liquids*, 279, 251–266. <https://doi.org/10.1016/j.molliq.2019.01.113>
- Andrew, J. J., Srinivasan, S. M., Arockiarajan, A., & Dhakal, H. N. (2019). Parameters influencing the impact response of fiber-reinforced polymer matrix composite materials: A critical review. *Composite Structures*, 224, 111007. <https://doi.org/10.1016/J.COMPSTRUCT.2019.111007>
- Babu, N. S. M., Mathivanan, N. R., & Kumar, K. V. (2019). Influence of machining parameters on the response variable during drilling of the hybrid laminate. *Australian Journal of Mechanical Engineering*. <https://doi.org/10.1080/14484846.2019.1704492>
- Bagci, E., & Yüncüoğlu, E. U. (2017). The effects of milling strategies on forces, material removal rate, tool deflection, and surface errors for the rough machining of complex surfaces. *Strojniski Vestnik/Journal of Mechanical Engineering*, 63(11), 643–656. <https://doi.org/10.5545/sv-jme.2017.4450>
- Bucholz, E. W., Phillpot, S. R., & Sinnott, S. B. (2012). Molecular dynamics investigation of the lubrication mechanism of carbon nano-onions. *Computational Materials Science*, 54(1), 91–96. <https://doi.org/10.1016/j.commatsci.2011.09.036>
- Camisasca, A., & Giordani, S. (2017). Carbon nano-onions in biomedical applications: Promising theranostic agents. In *Inorganica Chimica Acta* (Vol. 468, pp. 67–76). Elsevier S.A. <https://doi.org/10.1016/j.ica.2017.06.009>
- Cha, J., Kim, J., Ryu, S., & Hong, S. H. (2019). Comparison to mechanical properties of epoxy nanocomposites reinforced by functionalized carbon nanotubes and graphene nanoplatelets. *Composites Part B: Engineering*, 162, 283–288. <https://doi.org/10.1016/j.compositesb.2018.11.011>
- Chandrasekhar, S., & Prasad, N. (2020). Multi-response optimization of electrochemical machining parameters in the micro-drilling of AA6061-TiB<sub>2</sub> in situ composites using the Entropy–VIKOR method: <https://doi.org/10.1177/0954405420911539>, 234(10), 1311–1322. <https://doi.org/10.1177/0954405420911539>
- Chate, G. R., Patel, G. C. M., Bhushan, S. N. B., Parappagoudar, M. B., & Deshpande, A. S. (2019). Comprehensive modelling, analysis and optimization of furan resin-based moulding sand system with sawdust as an additive. *Journal of the Brazilian Society of Mechanical Sciences and Engineering*, 41(4), 0–24. <https://doi.org/10.1007/s40430-019-1684-0>
- Chau, N. Le, Nguyen, M.-Q., Dao, T.-P., Huang, S.-C., Hsiao, T.-C., Dinh-Cong, D., & Dang, V. A. (2018). An effective approach of adaptive neuro-fuzzy inference system-integrated teaching learning-based optimization for use in machining optimization of S45C CNC turning. *Optimization and Engineering* 2018 20:3, 20(3), 811–832. <https://doi.org/10.1007/S11081-018-09418-X>
- Chen, J., Tuo, W., Wei, P., Okabe, Y., Xu, M., & Xu, M. (2017). Characteristics of the shear mechanical properties and the influence mechanism of short basalt fiber reinforced polymer composite materials: <https://doi.org/10.1177/1099636217716466>, 21(4), 1520–1534. <https://doi.org/10.1177/1099636217716466>

- Cheng, D. J., Xu, F., Xu, S. H., Zhang, C. Y., Zhang, S. W., & Kim, S. J. (2020). Minimization of Surface Roughness and Machining Deformation in Milling of Al Alloy Thin-Walled Parts. *International Journal of Precision Engineering and Manufacturing*, 21(9), 1597–1613. <https://doi.org/10.1007/s12541-020-00366-0>
- Davim, J. P., & Reis, P. (2005). Damage and dimensional precision on milling carbon fiber-reinforced plastics using design experiments. *Journal of Materials Processing Technology*, 160(2), 160–167. <https://doi.org/10.1016/j.jmatprotec.2004.06.003>
- Desai, C. K., & Shaikh, A. (2012). Prediction of depth of cut for single-pass laser micro-milling process using semi-analytical, ANN and GP approaches. *International Journal of Advanced Manufacturing Technology*, 60(9–12), 865–882. <https://doi.org/10.1007/s00170-011-3677-8>
- Dhand, V., Mittal, G., Rhee, K. Y., Park, S. J., & Hui, D. (2015). A short review on basalt fiber reinforced polymer composites. *Composites Part B: Engineering*, 73, 166–180. <https://doi.org/10.1016/j.compositesb.2014.12.011>
- Dhand, V., Yadav, M., Kim, S. H., & Rhee, K. Y. (2021). A comprehensive review on the prospects of multi-functional carbon nano onions as an effective, high-performance energy storage material. *Carbon*, 175, 534–575. <https://doi.org/10.1016/j.carbon.2020.12.083>
- Ebrahimnejad, S., Mousavi, S. M., Tavakkoli-Moghaddam, R., & Heydar, M. (2012). Evaluating high risks in large-scale projects using an extended VIKOR method under a fuzzy environment. *International Journal of Industrial Engineering Computations*, 3(3), 463–476. <https://doi.org/10.5267/J.IJIEC.2011.12.001>
- Fu, G., Huo, D., Shyha, I., Pancholi, K., & Alzahrani, B. (2020). Experimental investigation on micromachining of epoxy/graphene nano platelet nanocomposites. *International Journal of Advanced Manufacturing Technology*, 107(7–8), 3169–3183. <https://doi.org/10.1007/s00170-020-05190-4>
- Ghafari-zadeh, S., Chatelain, J. F., & Lebrun, G. (2016). Finite element analysis of surface milling of carbon fiber-reinforced composites. *International Journal of Advanced Manufacturing Technology*, 87(1–4), 399–409. <https://doi.org/10.1007/s00170-016-8482-y>
- Gupta, M. K., & Srivastava, R. K. (2016). Mechanical Properties of Hybrid Fibers-Reinforced Polymer Composite: A Review. <http://Dx.Doi.Org/10.1080/03602559.2015.1098694>, 55(6), 626–642. <https://doi.org/10.1080/03602559.2015.1098694>
- Han, X., Zhao, Y., Sun, J. M., Li, Y., Zhang, J. D., & Hao, Y. (2017). Effect of graphene oxide addition on the interlaminar shear property of carbon fiber-reinforced epoxy composites. *Xinxing Tan Cailiao/New Carbon Materials*, 32(1), 48–55. [https://doi.org/10.1016/S1872-5805\(17\)60107-0](https://doi.org/10.1016/S1872-5805(17)60107-0)
- Harii Krishna Rao, G., Ansari, M. N. M. M., Rao, G., & Ansari, M. N. M. M. (2012). Effect of cutting parameters on the surface roughness of MWCNT reinforced epoxy composite using end-milling process. *Technical Proceedings of the 2012 NSTI Nanotechnology Conference and Expo, NSTI-Nanotech 2012*, 2(11), 252–255.
- He, Y., Qing, H., Zhang, S., Wang, D., & Zhu, S. (2017). The cutting force and defect analysis in milling of carbon fiber-reinforced polymer (CFRP) composite. *International Journal of Advanced Manufacturing Technology*, 93(5–8), 1829–1842. <https://doi.org/10.1007/s00170-017-0613-6>
- Hussain, G., Al-Ghamdi, K. A., Bijanrostami, K., & Alehashemi, A. J. (2016). Determination of Optimum Process Parameters for Cutting Hole in a Randomly-oriented Glass Fiber Reinforced Epoxy Composite by Milling Process: Maximization of Surface Quality and Cut-hole Strength. *Polymers and Polymer Composites*, 24(2), 81–89. <https://doi.org/10.1177/096739111602400201>
- Jenarthanan, M. P., Prakash, A. L., & Jeyapaul, R. (2016). Mathematical modeling of delamination factor on end milling of hybrid GFRP composites through RSM. *Pigment and Resin Technology*, 45(5), 371–379. <https://doi.org/10.1108/PRT-08-2015-0083>
- Jenkins, P., Siddique, S., Khan, S., Usman, A., Starost, K., MacPherson, A., Bari, P., Mishra, S., & Njuguna, J. (2019). Influence of Reduced Graphene Oxide on Epoxy/Carbon Fiber-Reinforced Hybrid Composite: Flexural and Shear Properties under Varying Temperature Conditions. *Advanced Engineering Materials*, 21(6). <https://doi.org/10.1002/adem.201800614>
- Kostagiannakopoulou, C., Tsilimigkra, X., Sotiriadis, G., & Kostopoulos, V. (2017). Synergy effect of carbon nano-fillers on the fracture toughness of structural composites. *Composites Part B: Engineering*, 129, 18–25. <https://doi.org/https://doi.org/10.1016/j.compositesb.2017.07.012>
- Krishnaraj, V., Prabukarthi, A., Ramanathan, A., Elanghovan, N., Kumar, M. S., Zitoune, R., & Davim, J. P. (2012). Optimization of machining parameters at high speed drilling of carbon fiber reinforced plastic (CFRP) laminates. *Composites Part B: Engineering*, 43(4), 1791–1799. <https://doi.org/10.1016/j.compositesb.2012.01.007>
- Kristianto, H., Putra, C. D., Arie, A. A., Halim, M., & Lee, J. K. (2015). Synthesis and Characterization of Carbon Nanospheres Using Cooking Palm Oil as Natural Precursors onto Activated Carbon Support. *Procedia Chemistry*, 16, 328–333. <https://doi.org/10.1016/j.proche.2015.12.060>
- Kuilla, T., Bhadra, S., Yao, D., Kim, N. H., Bose, S., & Lee, J. H. (2010). Recent advances in graphene based polymer composites. In *Progress in Polymer Science (Oxford)* (Vol. 35, Issue 11, pp. 1350–1375). Elsevier Ltd. <https://doi.org/10.1016/j.progpolymsci.2010.07.005>
- Kumar, D., & Singh, K. K. (2016). An experimental investigation of surface roughness in the drilling of MWCNT doped carbon/epoxy polymeric composite material. *IOP Conference Series: Materials Science and Engineering*, 149(1), 012096. <https://doi.org/10.1088/1757-899X/149/1/012096>
- Kumar, Dhiraj, & Gururaja, S. (2020). Machining damage and surface integrity evaluation during milling of UD-CFRP laminates: Dry vs. cryogenic. *Composite Structures*, 247(May), 112504.

- <https://doi.org/10.1016/j.compstruct.2020.112504>
- Kumar, V., Diyaley, S., & Chakraborty, S. (2020). Teaching-Learning-Based Parametric Optimization of An Electrical Discharge Machining Process. *Facta Universitatis, Series: Mechanical Engineering*, 18(2), 281–300. <https://doi.org/10.22190/FUME200218028K>
- Lau, K. tak, Gu, C., & Hui, D. (2006). A critical review on nanotube and nanotube/nanoclay related polymer composite materials. *Composites Part B: Engineering*, 37(6), 425–436. <https://doi.org/10.1016/j.compositesb.2006.02.020>
- Mangalgi, P. D. (1999). Composite materials for aerospace applications. *Bulletin of Materials Science* 1999 22:3, 22(3), 657–664. <https://doi.org/10.1007/BF02749982>
- Mittal, G., Dhand, V., Rhee, K. Y., Park, S. J., & Lee, W. R. (2015). A review on carbon nanotubes and graphene as fillers in reinforced polymer nanocomposites. *Journal of Industrial and Engineering Chemistry*, 21(March), 11–25. <https://doi.org/10.1016/j.jiec.2014.03.022>
- Opricovic, S., & Tzeng, G. H. (2007). Extended VIKOR method in comparison with outranking methods. *European Journal of Operational Research*, 178(2), 514–529. <https://doi.org/10.1016/J.EJOR.2006.01.020>
- Paulo Davim, J., Silva, L. R., Festas, A., & Abrão, A. M. (2009). Machinability study on precision turning of PA66 polyamide with and without glass fiber reinforcing. *Materials and Design*, 30(2), 228–234. <https://doi.org/10.1016/j.matdes.2008.05.003>
- Phiri, J., Gane, P., & Maloney, T. C. (2017). General overview of graphene: Production, properties and application in polymer composites. In *Materials Science and Engineering B: Solid-State Materials for Advanced Technology* (Vol. 215, pp. 9–28). Elsevier Ltd. <https://doi.org/10.1016/j.mseb.2016.10.004>
- Pikhurov, D., & Zuev, V. (2016). The Study of Mechanical and Tribological Performance of Fulleroid Materials Filled PA 6 Composites. *Lubricants*, 4(2), 13. <https://doi.org/10.3390/lubricants4020013>
- Pikhurov, D. V., & Zuev, V. V. (2014). The effect of fullerene C60 on the dielectric behaviour of epoxy resin at low nanofiller loading. *Chemical Physics Letters*, 601, 13–15. <https://doi.org/10.1016/j.cplett.2014.03.056>
- Priti, Singh, M., & Singh, S. (2021). Micro-Machining of CFRP composite using electrochemical discharge machining and process optimization by Entropy-VIKOR method. *Materials Today: Proceedings*, 44, 260–265. <https://doi.org/10.1016/j.matpr.2020.09.463>
- Raghu, A. V., Karuppanan, K. K., & Pullithadathil, B. (2019). Highly Surface Active Phosphorus-Doped Onion-Like Carbon Nanostructures: Ultrasensitive, Fully Reversible, and Portable NH 3 Gas Sensors . *ACS Applied Electronic Materials*, 1(11), 2208–2219. <https://doi.org/10.1021/acsaelm.9b00412>
- Rajesh Mathivanan, N., Mahesh, B. S., & Anup Shetty, H. (2016). An experimental investigation on the process parameters influencing machining forces during milling of carbon and glass fiber laminates. *Measurement: Journal of the International Measurement Confederation*, 91, 39–45. <https://doi.org/10.1016/j.measurement.2016.04.077>
- Rao, R. V., & Patel, V. (2012). An elitist teaching-learning-based optimization algorithm for solving complex constrained optimization problems. *International Journal of Industrial Engineering Computations*, 3(4), 535–560. <https://doi.org/10.5267/J.IJIEC.2012.03.007>
- Rao, R. V., Savsani, V. J., & Vakharia, D. P. (2011). Teaching-learning-based optimization: A novel method for constrained mechanical design optimization problems. *Computer-Aided Design*, 43(3), 303–315. <https://doi.org/10.1016/J.CAD.2010.12.015>
- Ravi Sankar, B., & Umamaheswarrao, P. (2018). Multi objective optimization of CFRP Composite Drilling Using Ant Colony Algorithm. *Materials Today: Proceedings*, 5(2), 4855–4860. <https://doi.org/10.1016/j.matpr.2017.12.061>
- Richard, J., & Giandomenico, N. (2018). Electrode Profile Prediction and Wear Compensation in EDM-milling and Micro-EDM-Milling. *Procedia CIRP*, 68(April), 819–824. <https://doi.org/10.1016/j.procir.2017.12.162>
- Rodríguez-González, J. A., Rubio-González, C., Jiménez-Mora, M., Ramos-Galicia, L., & Velasco-Santos, C. (2018). Influence of the Hybrid Combination of Multiwalled Carbon Nanotubes and Graphene Oxide on Interlaminar Mechanical Properties of Carbon Fiber/Epoxy Laminates. *Applied Composite Materials*, 25(5), 1115–1131. <https://doi.org/10.1007/s10443-017-9656-y>
- Sahu, A. K., Thomas, J., & Mahapatra, S. S. (2020). An intelligent approach to optimize the electrical discharge machining of titanium alloy by simple optimization algorithm. *Proceedings of the Institution of Mechanical Engineers, Part E: Journal of Process Mechanical Engineering*. <https://doi.org/10.1177/0954408920964685>
- Sait, A. N. (2010). Optimization of machining parameters of GFRP pipes using evolutionary techniques. *International Journal of Precision Engineering and Manufacturing*, 11(6), 891–900. <https://doi.org/10.1007/s12541-010-0108-y>
- Samson, R. M., Rajak, S., Kannan, T. D. B., & Sampreet, K. R. (2020). Optimization of Process Parameters in Abrasive Water Jet Machining of Inconel 718 Using VIKOR Method. *Journal of The Institution of Engineers (India): Series C*, 101(3), 579–585. <https://doi.org/10.1007/s40032-020-00569-4>
- Shadab, M., Singh, R., & Rai, R. N. (2019). Multi-objective Optimization of Wire Electrical Discharge Machining Process Parameters for Al5083/7% B 4C Composite Using Metaheuristic Techniques. *Arabian Journal for Science and Engineering*, 44(1), 591–601. <https://doi.org/10.1007/s13369-018-3491-9>
- Sharma, N., Ahuja, N., Goyal, R., & Rohilla, V. (2020). Parametric optimization of EDD using RSM-Grey-TLBO-based MCDM approach for commercially pure titanium. *Grey Systems: Theory and Application*, 10(2), 231–245. <https://doi.org/10.1108/gs-01-2020-0008>
- Shokrieh, M. M., & Omid, M. J. (2009). Investigation of strain rate effects on in-plane shear properties of glass/epoxy composites. *Composite Structures*, 91(1), 95–102. <https://doi.org/10.1016/J.COMPSTRUCT.2009.04.035>

- Taheri-Behrooz, F., Esmkhani, M., & Yaghoobi-Chatroodi, A. (2020). Effect of testing procedure on the in-plane shear properties of CNF/glass/epoxy composites. *Polymers and Polymer Composites*, 28(3), 159–169. <https://doi.org/10.1177/0967391119867200>
- Thakur, R. K., & Singh, K. K. (2021). Influence of fillers on polymeric composite during conventional machining processes: a review. *Journal of the Brazilian Society of Mechanical Sciences and Engineering*, 43(2), 1–20. <https://doi.org/10.1007/s40430-021-02813-z>
- Vijayan, D., & Rajmohan, T. (2019). Modeling and evolutionary computation on drilling of carbon fiber-reinforced polymer nanocomposite: an integrated approach using RSM based PSO. *Journal of the Brazilian Society of Mechanical Sciences and Engineering*, 41(10), 395. <https://doi.org/10.1007/s40430-019-1892-7>
- Voss, R., Seeholzer, L., Kuster, F., & Wegener, K. (2017). Influence of fibre orientation, tool geometry and process parameters on surface quality in milling of CFRP. *CIRP Journal of Manufacturing Science and Technology*, 18, 75–91. <https://doi.org/10.1016/j.cirpj.2016.10.002>
- Xu, X., Wang, G., Wan, G., Shi, S., Hao, C., Tang, Y., & Wang, G. (2020). Magnetic Ni/graphene connected with conductive carbon nano-onions or nanotubes by atomic layer deposition for lightweight and low-frequency microwave absorption. *Chemical Engineering Journal*, 382, 122980. <https://doi.org/10.1016/j.cej.2019.122980>
- Yang, X., Lin, X., Li, M., & Jiang, X. (2020). Experimental Study on Surface Integrity and Kerf Characteristics During Abrasive Waterjet and Hybrid Machining of CFRP Laminates. *International Journal of Precision Engineering and Manufacturing*, 21(12), 2209–2221. <https://doi.org/10.1007/s12541-020-00415-8>
- Yao, Y., Zhu, D., Zhang, H., Li, G., & Mobasher, B. (2016). Tensile Behaviors of Basalt, Carbon, Glass, and Aramid Fabrics under Various Strain Rates. *Journal of Materials in Civil Engineering*, 28(9), 04016081. [https://doi.org/10.1061/\(ASCE\)MT.1943-5533.0001587](https://doi.org/10.1061/(ASCE)MT.1943-5533.0001587)
- Yu, Y. H., Lin, Y. Y., Lin, C. H., Chan, C. C., & Huang, Y. C. (2014). High-performance polystyrene/graphene-based nanocomposites with excellent anti-corrosion properties. In *Polymer Chemistry* (Vol. 5, Issue 2). <https://doi.org/10.1039/c3py00825h>
- Zhou, J., Ren, J., & Yao, C. (2017). Multi-objective optimization of multi-axis ball-end milling Inconel 718 via grey relational analysis coupled with RBF neural network and PSO algorithm. *Measurement: Journal of the International Measurement Confederation*, 102, 271–285. <https://doi.org/10.1016/j.measurement.2017.01.057>



© 2022 by the authors; licensee Growing Science, Canada. This is an open access article distributed under the terms and conditions of the Creative Commons Attribution (CC-BY) license (<http://creativecommons.org/licenses/by/4.0/>).